Analytical Methods

PAPER

Cite this: *Anal. Methods*, 2018, **10**, 1038

Direct analysis in real time mass spectrometry (DART-MS) of discrete sample areas without heat damage†

G. Asher Newsome, *[a] Ikumi Kayama [b] and Shannon A. Brogdon-Grantham [a]

Received 28th December 2017
Accepted 6th February 2018

DOI: 10.1039/c7ay02987j

rsc.li/methods

Direct analysis in real time mass spectrometry (DART-MS) analyzes intact object surfaces by exposing them to a stream of heated gas. The continuous gas flow prevents discrete sampling of a central surface area, and the high temperatures cause visible discoloration and deformation of heat-sensitive materials. A time-controlled mechanical shutter was installed in front of a DART ion source mounted at an angle to the ion inlet for discrete sample surface analyses. Interior areas on stationary surfaces were studied without exposing the surrounding material of the greater object. The temperature exposure profile and spatial dimensions of areas impacted by the heated ionization gas were characterized to optimize DART positioning. Physical effects from DART of thermally sensitive photographs were recorded at various exposure times and temperatures, and high resolution mass spectra were acquired without causing visible or microscopic damage to photograph images. The shutter afforded 0.25 s DART-MS analysis time that was as qualitatively informative as exposures for tens of seconds.

Introduction

Mass spectrometry (MS) provides the most specific analysis of objects but commonly requires physically sectioning sample material, and such destructive testing is generally a last resort when the object of interest is rare or valuable. Pyrolysis with gas chromatography-MS consumes mg amounts of sample that must be cut from a whole object.[1] Laser desorption/ionization MS samples an area tens of μm in diameter,[2] and secondary ion MS uses an ion beam that sputters material from an area several nm in diameter,[3,4] but both methods require a section of the sample to fit inside a vacuum chamber. Unlike longer-established methods, ambient mass spectrometry analyzes intact object surfaces without sample sectioning or other preparation and is operated outside a vacuum chamber,[5] but visual and microscopic damage can also result. Desorption electrospray ionization causes little or no damage to metal and hard solids, but positioning the needle closer to the sample surface for higher spatial resolution and signal abundance ablates softer material.[6,7] Direct analysis in real time (DART) thermally desorbs material from sample surfaces using at minimum 50 °C but often hundreds of degrees Celsius[8,9] that can cause discoloration, melting, and burning.[10–13] Low temperature plasma (LTP) MS poses less risk of heat damage,[14] but desorbing less material with lower temperatures necessarily produces less ion signal.[15] LTPs have been used for conservation work,[16,17] but depending on the exposure time damage can be caused such as yellowing of paper,[18] micro-etching of metal,[19] and degradation of animal[20] and plant fibers.[21]

Regardless of the potential for heat damage, DART ionization is versatile for analysis of different materials because it can be operated at different temperatures. The commercial DART ion source flows a plume of gas continuously at the sample, transfer tube, and ion inlet.[9] Ionization cannot be instantly activated at a controlled temperature without first flowing gas for some minutes while the gas cell is heated to the temperature set-point. If the sample is placed in position before turning on the gas flow, the analysis area is exposed to slowly increasing temperatures that thermally desorb and deplete analyte before the optimum set-point is reached. Samples are moved manually or robotically into and out of the DART gas plume after the temperature has stabilized at the set-point.[9] In transmission mode DART where the heated gas plume is directed straight at the transfer tube, no more than the edge of a solid object may be analyzed without obstructing gas flow and decreasing signal,[22] unless part of object is cut away for analysis.[23] Intact objects larger than ~1 cm in more than one dimension are analyzed by reflection mode (also referred to as "surface desorption mode" and "desorption at an angle") DART, in which the heated gas plume is directed at an angle to the object surface.[24] A central point on an object surface may be analyzed as well as an edge, but the sample must be moved into position while outer surface area is indiscriminately exposed to the heated gas. The sample

[a]*Smithsonian Institution, Museum Conservation Institute, Suitland, MD 20746-2863, USA. E-mail: newsomeg@si.edu; Fax: +1 301-238-3709; Tel: +1 301-238-1223*

[b]*Studio Kayama, Riverdale, MD 20737-1330, USA*

† Electronic supplementary information (ESI) available. See DOI: 10.1039/c7ay02987j

surface is also exposed to a distribution of temperatures[25] as it moves across the DART gas plume.

Here, a DART ion source is converted into a discrete ambient MS sampling system by the addition of an external shutter. The shutter remains closed until a stationary, centrally-located sample area is in position for reflection mode DART analysis, after which the shutter opens for a set time. Every part of the analysis area is exposed to a constant temperature for the duration of the analysis. Each factor affecting the analysis is individually optimized without exposing peripheral areas of the sample surface. Exposure time and temperature are finely tuned to produce maximum ion signal from thermally sensitive photographs[26–28] with minimal or no visual or microscopic damage to the sample.

Experimental

Instrumental configuration

A DART-100 probe using helium discharge gas and operated by a SVP controller (IonSense, Saugus, MA) was custom-mounted to interface to a LTQ Orbitrap Velos mass spectrometer (Thermo Fisher Scientific, Waltham, MA). A 30 cm ruled crossbar was held by shaft collars between two upright 90 cm posts mounted independently from and at the base of the mass spectrometer. Housing and shielding were removed from the DART cell, which was suspended from above by multi-dimensional translation stages on the crossbar. An IonSense Vapur flange differentially pumped by a MZ2NT diaphragm pump (Vacuubrand, Essex, CT) was installed over the mass spectrometer heated ion inlet. A ceramic transfer tube 67 mm in total length extended 40 mm from the Vapur flange.

The DART cell was aligned laterally with the center of the ceramic transfer tube and ion inlet in the x dimension and set 45° to normal for reflection mode analysis (Fig. 1). The ceramic cap on the DART cell was tapered[29,30] to a flat 2.5 mm plane with a centered exit orifice 0.5 mm in diameter. With the angled cell, the ceramic edge extended 0.7 mm forward of and 0.7 mm below the origin of the ionizing gas flow. A platform on independent translation stages was mounted 0.5 mm below the ceramic transfer tube to manipulate flat samples and the flat, tangential surface of irregularly-shaped samples underneath the DART gas plume. The platform and sample surfaces were positioned no higher than bottom of the transfer tube so that central points on samples could be analyzed. The DART mounting stages were adjusted in 2.5 mm increments to various positions denoted by height y above the sample platform ($y = 0$) and in-line distance z from the transfer tube ($z = 0$). The ceramic cap was directed toward the same position on the sample platform when moved at equal Δy and Δz distance.

For all experiments an SH-10 shutter (Electro-optical Products Corp., Ridgewood, NY) was mounted with the aluminum vane in the space between the platform and the transfer tube. The shutter covered an area of 225 mm^2 and was 0.25 mm thick. The diamond-shaped shutter was also centered on the transfer tube in the x dimension (when closed) and was translated in the z dimension in accordance with the DART ceramic cap relative to the transfer tube. In swinging open on a 35° arc from under the transfer tube and ceramic cap, the shutter moved 0.4 mm higher from the sample surface it covered. Each shutter movement open or closed was completed in 70 ms after being triggered. Programmable Arduino control[31] of a relay power supply to the shutter left it normally closed and opened for a period of time defined in milliseconds. All operations were defined by the shutter opening to expose sample surfaces for periods of 0.25 s to 20 s.

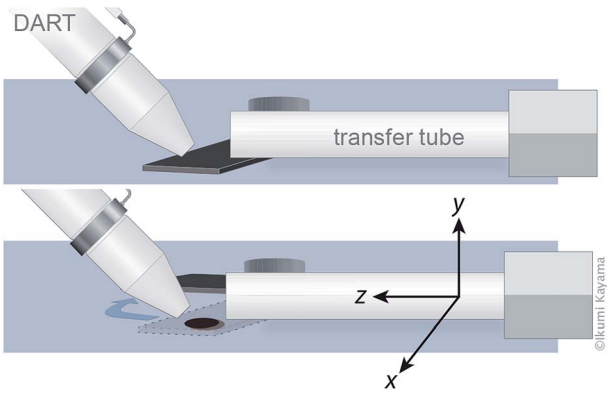

Fig. 1 Diagrams of DART cell mounted from above in reflection mode, with the shutter vane positioned between the DART ceramic cap/ceramic transfer tube and the sample surface (top), and swung open to expose the sample surface (bottom). Image ©ikumi kayama.

Temperature and sample analysis

Temperatures at sample surfaces were measured with a K-type thermocouple that had a junction 0.7 mm wide. The junction was passed through a hole in the platform when no sample was in place, extending 0.5 mm above the platform surface, below the shutter, transfer tube, and ceramic cap. Temperatures during 20 s shutter exposures from the DART were recorded once per second.

Thermal paper was also used as a visual indicator of temperature exposure. Pieces of thermal paper (RTUI, Houston, TX) were placed flat on the sample platform beneath the shutter for DART analysis. Fourier transform (FT) data was collected during various exposure times with 30 000 resolving power and 100 ms maximum fill times for a data point every 0.53 seconds on average. Prints produced by exposing thermochromic leuco dye on the paper to the DART plasma plume were scanned at 1200 dpi alongside a ruler. Prints were adjusted and posterized by grayscale value using Photoshop (Adobe, San Jose, CA), and gray value dimensions were selected and measured. Separate pieces of thermal paper were placed in an oven for five minutes each at varying temperatures to develop the dye.

DART was used to analyze 12.4 × 9 cm resin-coated (RC) chromogenic photographs for various exposure times. Best practice for long-term dark storage of photographs is in an environment at 2 °C and 40% relative humidity.[32] The photographs analyzed had previously been stored in a container indoors, in the dark, and in otherwise unknown conditions for

eighteen to nineteen years. FT analysis of photographs was done with 7500 resolving power (reduced to maximize scan speed) and 100 ms maximum fill time for a data point every 0.24 seconds on average. Accordingly, the minimum exposure time programmed for the shutter was 0.25 s. Three different photographs were analyzed, and DART mass spectra were compared within individual prints. Photographs exposed to DART were examined with 50× and 150× magnification using a Hirox KH-8700 digital microscope (Hirox-USA, Hackensack, NJ) with a MXG-2500REZ lens using the co-axial light setting. The dimensions of physical deformation to the photograph from the DART exposure were measured with Photoshop.

Results

Thermocouple measurement

The temperature of the post-plasma gas plume to which ambient surfaces were exposed was significantly lower than the set-point because the helium cools rapidly upon exiting the DART cell. The most straight-forward method of measuring the temperature at the surface exposed to the DART gas plume is with an electronic sensor in place of a sample.[33,34] A thermocouple mounted on the sample platform was translated to different positions in the *xz* plane. With the shutter closed, the temperature directly underneath the shutter was at maximum 32 °C when the DART helium setting was 250 °C. The recorded temperature increased for the first four seconds after the shutter opened and stabilized around a final value, fluctuating ±2 °C for the remainder of a 20 s exposure. After the shutter closed the temperature decreased below 40 °C within 20 s. The flow dynamics produced a distribution of temperatures across the exposed sample surface (Fig. 2). Elevated temperatures were observed in a pattern elongated along the *z* axis, with the hottest part of the surface closer to the ceramic cap. The ceramic cap was set to different positions relative to the transfer tube in the *yz* plane. With the ceramic cap at *z* 0 mm and *y* 0.5 mm, the gas plume was directed at the surface area immediately below the lip of the transfer tube. The highest temperature at the surface recorded at any ceramic cap position was 145 °C with the DART helium setting at 250 °C and the shutter open (Fig. S1†). The maximum temperature was lower when the ceramic cap was closer to the transfer tube because the heated gas was removed from the thermocouple more efficiently. Heat transfer to the thermocouple was less efficient with the ceramic cap at greater height remove from the sample platform. Measured maximum temperatures were highly linear with the DART helium temperature setting, reading 45 °C and 250 °C at settings of 50 °C and 500 °C, respectively, with the ceramic cap at *z* 0 mm and *y* 0.5 mm.

z (mm)						
-0.5	44	42	40			
0	49	53	46			
0.5	65	68	55	38		
1.0	86	74	60	44		
1.5	96	84	61	45		
2.0	106	91	63	45	40	
2.5	117	95	65	43	41	
3.0	128	111	57	45	41	
3.5	138	124	57	45	40	
4.0	127	119	49	40		
4.5	88	81	43	40		
5.0	40	39	39			
	0	0.6	1.3	1.9	2.5	*x* (mm)

Fig. 2 Maximum temperature (°C) observed by surface-level thermocouple at various positions in the *xz* plane, with DART at helium temperature setting of 250 °C and positioned with 7.5 mm between ceramic cap and inlet tube and 0.5 mm height *y* above the sample surface. Positive *z* values denote the thermocouple distance from the lip of the transfer tube toward the DART ceramic cap; *x* values denote lateral distance from the center of the transfer tube.

Temperature visualization with thermal paper

Thermal paper coated with heat-activated leuco dye was used to visualize the surface impact and analysis area from the DART post-plasma plume of gas at various ceramic cap positions. The irreversible color change of thermal paper was an imprecise measurement of temperature but was more accurate than the surface-level thermocouple. In control experiments where thermal paper was heated in an oven, the minimum temperature for the dye to become visibly gray was 90 °C. The color value increased with temperature up to 140 °C, above which the color value was constant through 200 °C. At 220 °C the black thermal paper became tinged with orange. Dark thermal paper prints from the DART plume were created by exposures at every ceramic cap position for which the maximum temperature at the surface was measured by thermocouple in Fig. S1.† Many thermocouple measurements within the gas plume impact area were significantly lower than 140 °C, indicating that the thermocouple consistently under-represented the temperature at the surface exposed on a timescale of seconds. Well-formed thermal paper prints produced by exposures as short as 0.25 s also indicated that the speed of heat transfer was quicker than the thermocouple could measure. The thermocouple probe has greater mass in which to sink heat compared to the leuco dye on thermal paper and therefore registers a lower temperature more slowly.

DART analysis areas indicated by thermal paper prints were generally elliptical with the major axis along the *z* dimension between the ceramic cap and transfer tube (Fig. S2†). The most evenly colored, matte black prints were produced with the ceramic cap closer to the transfer tube. The transfer tube was a partial obstruction to the DART gas plume when the center of the analysis area was closer than 3 mm (positions $z \leq 2.5$ mm, *y* 0.5 mm; $z \leq 5$ mm, *y* 3 mm; $z \leq 7.5$ mm, *y* 5.5 mm), causing

asymmetry of thermal paper prints from heat distribution behind the lip of the transfer tube. With the ceramic cap at greater distance z from the transfer tube, prints had greater variation in shade because the analysis area temperature distribution was more gradual. The darkest part of a print, *i.e.* the hottest part within an analysis area, was closer to the ceramic cap as in the thermocouple measurement pattern of Fig. 2.

The dimensions of the analysis area exposed to the gas plume were a measure of the DART heat transfer efficiency, independent of the efficiency of ion detection. Thermal paper prints were compared for a variety of analysis area exposure times and ceramic cap positions relative to the transfer tube and sample surface (Fig. 3). Differences in print area as a function of ceramic cap position were most significant with a 20 s exposure time. At greater distance between the ceramic cap and the transfer tube, the reduced effect of the supplementary vacuum on the DART gas plume produced larger print areas. The supplementary vacuum had little to no effect on the gas plume beyond a central point in the z axis, and the print area was less likely to extend out of a smaller, more symmetrical ellipse. Greater height y above the sample surface produced smaller print areas because the DART gas plume dispersed with distance. Length and width measurements of prints (Fig. S3 and S4†) were proportional to measurements of total analysis area. The length and width of the thermal paper prints were greater than the dimensions of temperatures measured above 140 °C in Fig. 2, demonstrating that the thermocouple under-represented actual temperatures at the surface.

Shutter control of DART exposure resolved the time dependence of heat transfer to the sample surface. At a constant ceramic cap position, the area of thermal paper prints increased with DART exposure time up to 3 s but was not significantly different at longer exposure time (Fig. S5†). For 0.25 s exposures, there was no significant difference between analysis area prints as a function of ceramic cap position when the center of the analysis area was at least 3 mm from the transfer tube. The print produced by 0.25 s exposure was as symmetrical as the print produced by 20 s exposure (Fig. S6†). Because the heat transfer efficiency of 0.25 s DART experiments was independent of ceramic cap position, sub-2.5 mm precision in the y dimension would not be necessary for mounting an irregularly sized or textured sample surface.

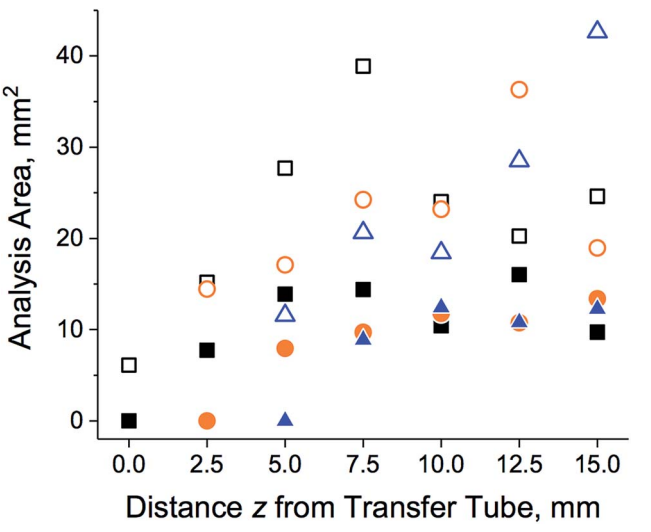

Fig. 3 Analysis area coverage by DART of thermal paper with a helium temperature setting of 250 °C, at various ceramic cap distances z from the transfer tube and heights y above the sample surface 0.5 mm (black squares), 3.0 mm (orange circles), and 5.5 mm (blue triangles) for sample exposures lasting 20 s (open symbols) and 0.25 s (filled symbols).

Mass spectral analysis of thermal paper

Unlike print area dimensional measurements, comparison of ion signal relative to ceramic cap position necessarily convolved thermal desorption efficiency and ion detection efficiency. Mass spectra were acquired from analysis of thermal paper at each ceramic cap position relative to the transfer tube and sample surface (Fig. S7†). Selected ion signals from 20 s exposures were compared to characterize different classes of analyte. Carboxin (m/z 236 and fragment ion m/z 219) was the most consistently observed analyte, accounting for at least one third of total ion signal. Although transmission mode DART analyses have been performed without memory effects,[35,36] exposure of thermal paper to the reflection mode DART gas plume readily caused carboxin to contaminate the transfer tube without physically contacting the thermal paper. Carboxin was observed for minutes after the shutter was closed and the thermal paper sample was removed. Contamination was removed by sonicating the transfer tube in methanol. When carboxin ions were included in the total, summed ion signal was largest with the ceramic cap was closest to the transfer tube (Fig. 4a) because analyte was desorbed from the thermal paper and the contaminated transfer tube.

There was no single mass spectrum wholly representative of DART ion signal because the relative abundance of many analyte ions changed over the 20 s exposure period. The change in signal abundance was not uniform relative to ceramic cap position for the various ions. The sum of analytes not including carboxin produced maximum signal when the ceramic cap was 5 to 7.5 mm from the transfer tube, as close as possible without obstructing the DART gas plume (Fig. 4b). Subdividing analytes further, signals that increased in abundance over time were greatest when the ceramic cap was closest to the sample surface and close to the transfer tube without obstruction to the DART gas plume (Fig. 4c). Ceramic cap position relates directly to temperature at the analyte surface. The majority of analytes produced maximum signal at the highest temperature, but some compounds were best observed at lower temperature. Analyte signal that decreased in abundance over the exposure period was greatest when the ceramic cap was farthest from the sample surface (Fig. 4d). Analytes with higher vapor pressure were more slowly depleted by lower temperatures and produced more ion signal over time. The range of temperatures produced by different ceramic cap positions was insufficient to alter analyte ion fragmentation.

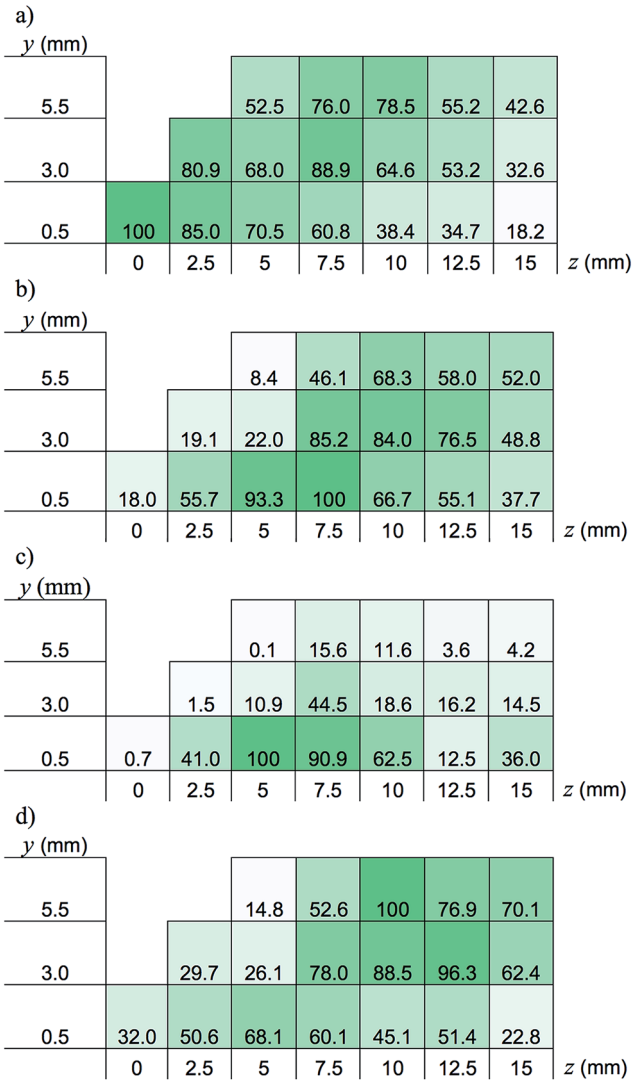

Fig. 4 Sum of ion signals observed by DART of thermal paper over 20 s exposure with a helium temperature setting of 250 °C at various ceramic cap distances *z* from the transfer tube and heights *y* above the sample surface, in relative terms: (a) total ion signal; (b) total ion signal excluding carboxin and fragment ion, *m/z* 236 and 219; (c) sum of signal from ions that increase in abundance over the exposure time, *m/z* 325, 268, and 251; and (d) sum of signal from ions that decrease in abundance over exposure time, *m/z* 404, 387, 346, 333, and 329.

Physical effects on RC chromogenic photographs from DART

RC chromogenic photographs were analyzed by DART in the position chosen for optimal overall ion signal and symmetrical analysis area, the ceramic cap 5 mm from the transfer tube and 0.5 mm above the sample surface. Contiguous photograph areas with evenly-hued blue color were exposed to the DART gas plume for various times and at various helium temperature settings. Photographs were translated 5 mm in *x* and 7.5 mm in *z* to prevent overlap of exposures, based on dimensions of thermal paper prints. With the DART helium set to 250 °C, exposure times from 0.25 s to 20 s caused visible damage to the analysis area of the photograph in the form of an elongated purple discoloration (Fig. S8†). Exposures for 3–20 s also caused physical warping to the photograph surface and visible damage to the paper on the reverse side. Visible under 50× magnification, the analysis areas had a physical deformation in the form of a highly symmetrical ellipse produced by the heat of the gas plume impact (Fig. S9†). The elliptical deformation area increased in size with DART exposure time up to 3 s but was not significantly larger at longer exposure time (Fig. S10†), the same pattern as the change in thermal paper print area as a function of exposure time. Photograph elliptical deformation was smaller than the corresponding thermal paper print because the photograph was visibly undamaged by the cooler outer part of the DART gas plume.

The hottest part of an analysis area, previously observed by thermocouple measurement in Fig. 2 and thermal paper shading in Fig. S2,† was characterized by a different type of physical deformation. Below the center of the ellipse formation was a smaller, roughly circular area with lines or cracks orthogonal to the major axis of the elliptical deformation. The indicator of maximum temperature was visible under magnification for all exposure times above 0.25 s. Darkening of the photograph surface was observed up to 0.4 mm outside the elliptical deformation along the border close to the ceramic cap. RC chromogenic photographs are composed of three layers of gelatin emulsion each containing cyan, magenta, and yellow azomethine or indoaniline dyes that form a subtractive color image, layered on top of a laminate support of paper fibers sandwiched between extruded polyethylene[37–39] (Fig. S11†). The dye-based gelatin emulsion layers are a few μm thick.[32] Areas of the photograph that were not exposed to the DART gas plume retained a sharp pattern of colored dye clouds and intact gelatin emulsion at 150× magnification. All parts of an analysis area within the elliptical deformation and the darkened region around its base had distorted dye clouds (Fig. S12†).

Damage to the photograph from 0.25 s exposure to DART gas was reduced or entirely eliminated by lowering the temperature. DART with a 350 °C helium setting pitted through the gelatin emulsion layers on the photograph surface to the pigmented polyethylene and/or paper layer, and 300 °C caused orthogonal deformation in the hottest part of the analysis area similar to longer exposure at lower temperature (Fig. 5). The area of the elliptical deformation directly decreased with temperature (Fig. S13†). The purple tint was barely perceptible on the blue image at 200 °C (Fig. S14†), and no discoloration was apparent to the naked eye with lower helium temperature setting. Magnification showed no surface damage in the form of elliptical deformation, shadowing, disruption to dye clouds, or otherwise for 100–150 °C temperature settings. No signs of visible damage became apparent 14 weeks after exposure. DART with lower helium temperature also prevented damage from longer exposures. No discoloration or deformation of the photograph as visible to the naked eye or under magnification was observed from 20 s exposure to 100 °C DART gas.

Mass spectral analysis of RC chromogenic photographs

Analyte ions were observed from all DART exposure of RC chromogenic photographs for 0.25 s or longer with helium

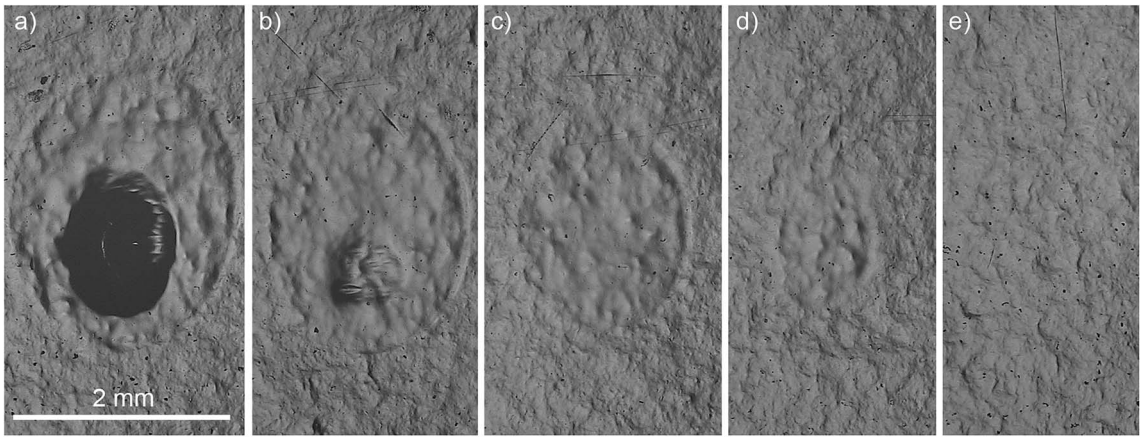

Fig. 5 Magnified gas plume impact areas on photograph exposed to DART for 0.25 s at helium temperature settings of (a) 350 °C, (b) 300 °C, (c) 250 °C, (d) 200 °C, and (e) (d) 150 °C with the ceramic cap at *z* 0 mm and *y* 0.5 mm. Analysis areas are not positioned identically within the images relative to the ceramic cap.

temperature settings of 100 °C or higher. The protonated molecule of dibutyl phthalate ($[C_{16}H_{23}O_4]^+$) was observed at *m*/*z* 279 (Fig. S15†) because the substance was used as a protection oil for dye couplers dispersed in the gelatin layers of the photographs. Dye couplers react with color-developing chemicals during photograph development processing, and the presence of dibutyl phthalate is the result of unreacted or residual couplers.[40] The dibutyl phthalate contaminated the transfer tube similar to carboxin from thermal paper and was omitted from ion signal comparisons. Ion signal increased with helium temperature setting above 150 °C, and the relative standard deviation between replicate analyses was unchanged (Fig. 6). The ion signal was equal for 0.25 s exposures with 100 °C and 150 °C temperature settings, the conditions where DART caused no visible damage to the photographic surface. The most abundant analyte ions were oxygen-containing amines, chemicals used in the proprietary processes that created the photograph. Similar to dibutyl phthalate, oxygen-containing amines may be part of the dye coupler structure or the dye itself.[40] Such DART signal could be used to identify chemical markers of degradation (such as dye color shift) of photographs by the blend of proprietary dyes and other chemicals observed.

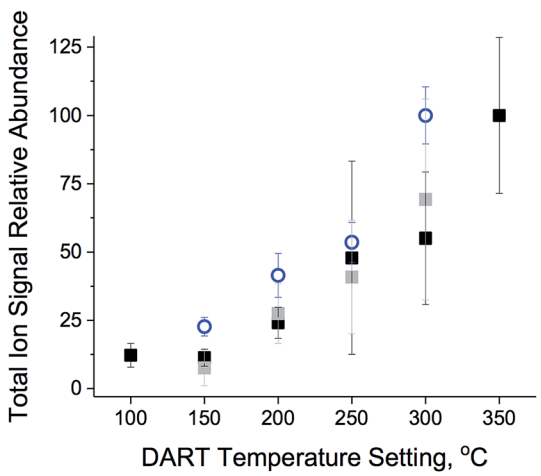

Fig. 6 Relative total ion signal abundance from replicate DART analyses of photograph surfaces with a helium temperature setting of 250 °C and the ceramic cap at *z* 0 mm and *y* 0.5 mm, reported as the average observed from a 0.25 s exposure (black filled squares), the average maximum value observed at any data point within a 20 s exposure (blue open circles), and the average value observed in the first data point in a 20 s exposure (gray filled squares) (standard deviation error bars).

The relative abundance of analyte ions changed over a 20 s exposure period. All ion signal decreased with increasing exposure time as analyte was depleted from the photograph surface (Fig. S16†). A single high-resolution mass spectrum could be acquired during a 0.25 s exposure, equivalent to the first data point recorded during a longer exposure (Fig. S15†). Mass spectra collected at different times within a 20 s DART analysis of a photograph were compared. The first data point from a sample exposure would be expected to contain the maximum ion signal. In practice, ion signal in some replicate analyses increased or was approximately constant for some amount of time before decreasing. The temperature dictated the length of time before the decrease in signal. Ion signal from the first mass spectrum was compared to the maximum ion signal observed from a single mass spectrum at any time during a 20 s exposure (Table 1). Rapid thermal desorption from the photograph surface produced more abundant ion signal for a shorter period of time. The likelihood that the first mass spectrum had the maximum ion signal increased with temperature. A 200 °C temperature setting or higher caused the first mass spectrum to have on average 70% the signal abundance of the maximum. The longest time elapsed before the maximum ion signal was observed was under three seconds at a 150 °C helium temperature setting. At all temperatures, a 0.25 s exposure was as useful for qualitative analysis as a 20 s exposure in addition to causing less physical damage to the sample. Replicates of 0.25 s DART analysis (five single data

Table 1 Photograph surface analysis replicates by 20 s exposure of DART with the ceramic cap at *z* 0 mm and *y* 0.5 mm, at various helium temperature settings (measurements ± standard deviation)

Temperature setting, deg. C	Percentage of replicate analyses where maximum signal was observed in the first data point	Average ratio of first data point signal to maximum signal observed during exposure	Average seconds into exposure window to observe maximum signal	Average sum of signal over entire exposure
150	0	0.3 ± 0.3	1.4 ± 1.5	$7.6 \times 10^5 \pm 5 \times 10^4$
200	20	0.7 ± 0.3	0.6 ± 0.4	$1.09 \times 10^6 \pm 5 \times 10^4$
250	40	0.7 ± 0.3	0.5 ± 0.3	$1.42 \times 10^6 \pm 8 \times 10^4$
300	40	0.7 ± 0.4	0.4 ± 0.1	$2.2 \times 10^6 \pm 1 \times 10^5$

points) had total ion signal relative standard deviation of 40% or more. The sum of ion signal from all mass spectra acquired from a single 20 s exposure (82 data points) had a relative standard deviation less than 6% over five replicates.

Conclusions

Precise control of sample exposure to the DART gas plume with a shutter eliminates heat damage while acquiring mass spectra from interior analysis areas on object surfaces. Every factor affecting reflection mode DART is optimized in discrete experiments: sample position on the platform, ceramic cap position relative to the sample and transfer tube, exposure time, and temperature. Measured dimensions of the analysis area and exposure temperatures more accurately represent the risk to the sample surface. Thermochromic dye prints from DART of thermal paper indicate wider exposure and higher peak temperatures than detectable with a thermocouple. When low-abundance analyte ion signal is not accompanied by higher-abundance ions, it is better discerned from background by the shutter opening at a programmed time. DART of photographs for 0.25 s with helium temperature settings of 100–150 °C produces qualitative mass spectral data without causing visible or microscopic damage to the heat-sensitive material, whereas the minimum temperature settings similar to LTP-MS produce no signal. Longer exposure times that produce less signal variability could be used for quantitative DART analysis.

Exposure temperature is the most important factor for DART analysis of thermally sensitive objects, but it cannot be accurately measured in a straightforward way. DART gas plume temperatures are commonly measured with an independent thermocouple, which underestimates the amount of heat exposure. Because various materials are susceptible to thermal desorption or heat damage at different temperatures, empirical measurements of reference materials are desirable to observe maximum ion signal without damaging a critical sample surface. Minimal exposure time and low temperature are necessary if the sample material is unknown or too rare for reference tests. If the risk of visible damage is a lower priority than mass spectral analysis, higher temperatures and longer exposure times can be used. Rough control of DART gas temperature settings in 50 °C increments is more finely tuned with limited exposure time and ceramic cap positioning. Longer exposure reduces the error bars for replicate analyses of samples that are not too rare for replicates. A shutter could be similarly installed to limit sample exposure to other post-plasma ambient ion sources. The rough temperature control of DART with the fine temperature and exposure manipulation of a shutter provide the most precise control for analysis of different materials.

Conflicts of interest

There are no conflicts to declare.

Acknowledgements

Thanks to Tim Cleland and Thomas Lam for helpful discussions, and thanks to Hansol America and RTUI, LP, for information about thermal paper.

References

1 A. M. Shedrinsky, T. P. Wampler, N. Indictor and N. S. Baer, *J. Anal. Appl. Pyrolysis*, 1989, **15**, 393–412.
2 D. S. Peterson, *Mass Spectrom. Rev.*, 2007, **26**, 19–34.
3 L. Van Vaeck, A. Adriaens and R. Gijbels, *Mass Spectrom. Rev.*, 1999, **18**, 1–47.
4 J. S. Fletcher, X. A. Conlan, E. A. Jones, G. Biddulph, N. P. Lockyer and J. C. Vickerman, *Anal. Chem.*, 2006, **78**, 1827–1831.
5 J. H. Gross, in *Mass Spectrometry-A Textbook*, Springer, Heidelberg, 2nd edn, 2011, pp. 621–648.
6 A. Venter, P. E. Sojka and R. G. Cooks, *Anal. Chem.*, 2006, **78**, 8549–8555.
7 The effect of nebulizing gas pressure, volumetric flow rate and tip-to-surface distance on spot size in DESI-MS, Prosolia Tech Note 117, 2007.
8 R. B. Cody, J. A. Laramee and H. D. Durst, *Anal. Chem.*, 2005, **77**, 2297–2302.
9 J. H. Gross, *Anal. Bioanal. Chem.*, 2014, **406**, 63–80.
10 M. Busman, J. H. Liu, H. J. Zhong, J. R. Bobell and C. M. Maragos, *Food Addit. Contam., Part A*, 2014, **31**, 932–939.
11 R. Williamson, A. Raeva and J. R. Almirall, *J. Forensic Sci.*, 2016, **61**, 706–714.

12 T. Trejos, P. Torrione, R. Corzo, A. Raeva, K. Subedi, R. Williamson, J. Yoo and J. Almirall, *J. Forensic Sci.*, 2016, **61**, 715–724.
13 J. M. Wells, M. J. Roth, A. D. Keil, J. W. Grossenbacher, D. R. Justes, G. E. Patterson and D. J. Barket Jr, *J. Am. Soc. Mass Spectrom.*, 2008, **19**, 1419–1424.
14 J. D. Harper, N. A. Charipar, C. C. Mulligan, X. Zhang, R. G. Cooks and Z. Ouyang, *Anal. Chem.*, 2008, **80**, 9097–9104.
15 J. Orejas, K. P. Pfeuffer, S. J. Ray, J. Pisonero, A. Sanz-Medel and G. M. Hieftje, *Anal. Bioanal. Chem.*, 2014, **406**, 7511–7521.
16 S. Voltolina, L. Nodari, C. Aibéo, E. Egel, M. Pamplona, S. Simon, E. V. Falzacappa, P. Scopece, A. Gambirasi and M. Favaro, *J. Cult. Herit.*, 2016, **22**, 940–950.
17 J. Szulc, W. Urbaniak-Domagałab, W. Machnowskib, H. Wrzosekb, Ł. Karolina and B. Gutarowskaa, *Int. Biodeterior. Biodegrad.*, 2017, DOI: 10.1016/j.ibiod.2017.01.021.
18 K. Pietrzak, A. Otlewska, D. Danielewicz, K. Dybka, D. Pangallo, L. Krakova, A. Puskarova, M. Buckova, V. Scholtz, M. Durovic, B. Surma-Slusarska, K. Demnerova and B. Gutarowska, *J. Cult. Herit.*, 2017, **24**, 69–77.
19 I. Turovets, M. Maggen and A. Lewis, *Stud. Conserv.*, 1998, **43**, 89–100.
20 S. Ratnapandian, L. Wang, S. M. Fergusson and M. Naebe, *J. Fiber Bioeng. Informat.*, 2011, **4**, 267–276.
21 X. Liu and L. Cheng, *J. Text. Inst.*, 2017, 1–6.
22 G. Morlock and Y. Ueda, *J. Chromatogr. A*, 2007, **1143**, 243–251.
23 D. Fraser, C. S. DeRoo, R. B. Cody and R. A. Armitage, *Analyst*, 2013, **138**, 4470–4474.
24 E. S. Chernetsova, A. I. Revelsky and G. E. Morlock, *Rapid Commun. Mass Spectrom.*, 2011, **25**, 2275–2282.
25 G. A. Newsome, L. K. Ackerman and K. J. Johnson, *Anal. Chem.*, 2014, **86**, 11977–11980.
26 J. E. LaBarca and S. F. O'Dell, in *lS&T's 12th International Symposium on Photofinishing Technology*, ed. S. Gordon, D. English and S. M. Howe, Ft, Lauderdale, FL, 2002, pp. 38–47.
27 P. Kozlov and G. Burdygina, *Polymer*, 1983, **24**, 651–666.
28 H. G. Wilhelm and C. Brower, in *The Permanence and Care of Color Photographs*, Preservation Publishing Company, Grinnell, Iowa, 1988.
29 T. T. Habe and G. E. Morlock, *Rapid Commun. Mass Spectrom.*, 2015, **29**, 474–484.
30 T. T. Habe and G. E. Morlock, *Rapid Commun. Mass Spectrom.*, 2016, **30**, 321–332.
31 https://github.com/nakulbende/TTL_Trigger, accessed 2017.
32 S. Pénichon and M. Jürgens, *Coatings on Photographs: Materials, Techniques, and Conservation, Photographic Material Groups*, American Institute for Conservation of Historic and Artistic Works, 2005.
33 M. N. Chan, T. Nah and K. R. Wilson, *Analyst*, 2013, **138**, 3749–3757.
34 R. K. Manova, S. Joshi, A. Debrassi, N. S. Bhairamadgi, E. Roeven, J. Gagnon, M. N. Tahir, F. W. Claassen, L. M. W. Scheres, T. Wennekes, K. Schroen, T. A. van Beek, H. Zuilhof and M. W. F. Nielen, *Anal. Chem.*, 2014, **86**, 2403–2411.
35 M. Zhou, J. F. McDonald and F. M. Fernandez, *J. Am. Soc. Mass Spectrom.*, 2010, **21**, 68–75.
36 M. E. Monge and F. M. Fernandez, *Ambient Ionization Mass Spectrometry*, ed. M. D. Domin and R. Cody, Royal Society of Chemistry, Cambridge, UK, 2015, pp. 1–22, ch. 1.
37 B. Lavédrine, *Photographs of the past: process and preservation*, Getty Publications, 2009.
38 S. Pénichon, *Twentieth-century color photographs: identification and care*, Getty Publications, 2013.
39 G. Weaver and Z. Long, in *Chromogenic characterisation: a study of Kodak color prints, 1942–2008*, PMG, Winter Meeting, 2009.
40 S. Fujita, *Organic Chemistry of Photography*, Springer, Berlin Heidelberg, 2004.